Konversi 15(1) (2026) 16-24

KONVERSI
Homepage:
https://ppjp.ulm.ac.id/journal/index.php/konversi

Process simulation of green ammonia production from oil palm frond (OPF) waste via gasification: A technical feasibility study

Rudy Heryadi*, Hendera

Department of Environmental Science, Faculty of Science and Technology, Universitas PGRI Kalimantan, Banjarmasin 70122, Indonesia

ARTICLE INFO

Article history:
Received: 05 January 2026
Received in revised form: 20 April 2026
Accepted: 20 April 2026

Keywords:

Ammonia, Biomass, gasification, OPF, simulation

ABSTRACT

Indonesia, as a leading palm oil producer, generates massive quantities of Oil Palm Frond (OPF) waste that are currently underutilized, particularly in Kalimantan. This study evaluates the technical feasibility of converting OPF into green ammonia as a sustainable energy alternative. The abundant availability of OPF in the Kalimantan region distinguishes this feedstock from generic woody biomass. A steady-state process simulation was developed to integrate gasification, syngas cleaning, water-gas shift (WGS), and ammonia synthesis. Using a feedstock input of 16,000 kg/h, the process yielded 8,381 kg/h of ammonia, achieving a biomass-to-ammonia ratio of 1.9:1 and a product purity of 97.18 mol% (equivalent to 98.57 wt%), meeting industrial standards for commercial applications. Plant performance analysis indicated an energy conversion efficiency of 55% and a specific energy consumption of 1.03 kWh/kg NH_3 across the compression and synthesis sections, representing only the thermodynamic potential of the core process. At the same time, the total facility-level energy demand, which accounts for the energy-intensive Air Separation Unit (ASU) and Pressure Swing Adsorption (PSA), is estimated to be significantly higher. These results confirm that the gasification of OPF is a technically viable pathway for green ammonia production, offering a promising solution for palm oil industry waste management and supporting the Indonesian government's national hydrogen and ammonia roadmap.

1. Introduction

Biomass is a raw material for several types of renewable energy and for various chemicals derived from it through conversion processes such as gasification, transesterification, and others. Biomass from palm oil waste, such as oil palm frond (OPF) and oil palm empty fruit bunches (OPEFB), can be converted into biofuels [1]. Palm oil industry waste has the potential to be used as a raw material for biofuel production, especially since Indonesia is the world's leading palm oil producer [1,2], particularly in Kalimantan and Sumatra.

According to Goh & Potter [2], OPF is one of the most abundant palm oil waste products. The potential for OPF waste in Kalimantan in 2019 was estimated at 19 million tonnes per year, far exceeding other types of palm oil industry waste [2]. OPF is a form of biomass that can be converted into fuel or biofuel through gasification. Gasification is a thermochemical process that converts biomass into a flammable gas, called producer gas, or a synthetic gas known as syngas. Syngas is a mixture of combustible gases composed primarily of hydrogen (H_2), carbon monoxide (CO), and methane (CH_4) [3]. Syngas is a raw material for many chemical products, including methanol, ammonia, and dimethyl ether (DME) [4,5]. Among those chemical products, ammonia (NH_3) can be used in a variety of applications, including as a fuel, refrigerant, fertilizer feedstock, and explosives [6–10].

Extensive research has established OPF as a promising renewable energy feedstock, with studies investigating its conversion into fuel pellets [11–13], bio-oil via pyrolysis [14–16], and bio-syngas through gasification [17–19]. Parallel to these feedstock-specific characterizations, the broader techno-economic feasibility of green ammonia production from biomass has been well documented; Andersson and Lundgren [20] and Gilbert et al. [21] have demonstrated the economic viability and carbon reduction potential of biomass gasification routes compared to conventional methods. Several other studies also explore the utilization of biomass to produce green ammonia, which is then used as a primary raw material in the fertilizer industry [22,23].

Beyond its traditional applications in fertilizers and explosives, green ammonia is emerging as a critical vector for the energy transition, serving both as a direct marine fuel and a high-density hydrogen carrier [24,25]. While its toxicity necessitates stringent safety protocols, ammonia offers a decisive logistical advantage over pure hydrogen, which requires energy-intensive storage at cryogenic temperatures (-253°C) or extreme pressures (70 MPa) [26]. Conversely, ammonia can be liquefied at moderate conditions and transported utilizing established global infrastructure, positioning it as a practical solution for long-distance renewable energy transport and maritime decarbonization [25–28].

Research on ammonia from biomass has been conducted from various perspectives, including techno-economic analysis,

* Corresponding author. Tel.: +6287775320179
Email: rudy.heryadi@breny.my.id
http://dx.doi.org/10.20527/k.v15i1.25112

This open access article is distributed under a Creative Commons Attribution (CC-BY-SA) 4.0 license

feasibility studies, process simulation, life cycle assessment, and estimation of biomass potential as a raw material for ammonia production [20–23,29–31]. Although many studies have been conducted, the technical feasibility of OPF-based ammonia remains unclear, especially in Indonesia, as the world's largest producer of palm oil and its waste.

Several studies have established the competitive potential of biomass-based ammonia. Gilbert et al. [21] demonstrated that substituting natural gas with woody biomass gasification could achieve greenhouse gas (GHG) savings of 65% and an Internal Rate of Return (IRR) of 9.8%, becoming cost-competitive at a carbon price of £32/tonne. Similarly, in a comparative study of feedstocks across Australia, Brazil, and India, Arora et al. [30] identified that while Indian straw offered the most economical scenario, Brazilian bagasse yielded the lowest GHG potential. Furthermore, Gençer et al. [22] addressed food security concerns, finding that only 1–5% of a grower's crop acreage is required to generate sufficient lignocellulosic biomass to meet nitrogen fertilizer needs.

Beyond feedstock selection, process configuration significantly impacts efficiency. Andersson & Lundgren [20] showed that integrating ammonia production into existing pulp and paper mills increased system efficiency to 54%, compared to 44% for stand-alone plants. Likewise, Martín and Sánchez [23] highlighted that integrating ammonia and urea production not only resolves CO_2 emissions but also stabilizes production costs. Regarding scale, Arora et al. [31] found that decentralized, small-scale biomass gasification is economically competitive, offering predicted CO_2 emission reductions of 54–68% compared to conventional plants.

Despite these advancements, the technical feasibility of utilizing Oil Palm Fronds (OPF) remains largely unexplored, particularly in Indonesia, the world's largest palm oil producer. To date, Heryadi et al. [29] provide the primary reference for this specific feedstock, estimating that Kalimantan has the potential to produce 22 million tonnes/year of OPF waste, which could theoretically yield 6.94 million tonnes of green ammonia. However, this study focused on potential estimation based on calorific value rather than a rigorous process simulation.

The primary benefit of this research is to determine the feasibility of converting abundant palm oil waste (OPF) that remains unutilized and creates a serious environmental problem year after year [27] into green ammonia, a potential substitute for fossil-fuel-based grey ammonia. Utilizing OPF, a palm oil waste product, as a raw material for green ammonia production can reduce GHG emissions and improve economic activity and the well-being of communities along the OPF-based green ammonia supply chain. The use of OPF as a feedstock for ammonia production also aligns with the Indonesian government's national hydrogen and ammonia roadmap, which includes the utilization of palm oil waste [32].

2. Method

The research stages can be described in Fig. 1 as follows.

2.1. Process simulation strategy

The ammonia production process from OPF was simulated using Aspen Hysys, a process engineering simulation software for plant and equipment design [33]. This simulation used a steady-state approach to evaluate the mass and energy balances throughout the plant.

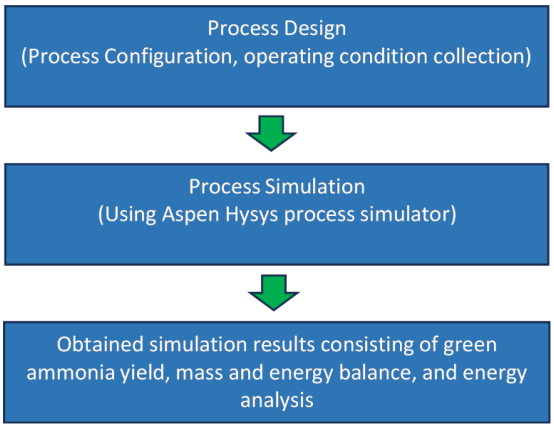

Fig. 1. Research stages description

The simulated OPF feedstock for ammonia production was assumed to be 16,000 kg/h, representing only 4.6% of the total OPF potential in South Kalimantan [29]. The Peng-Robinson (PR) equation of state was selected as the thermodynamic property package [34,35]. This fluid package is widely accepted in the petrochemical industry for modeling systems involving light gases such as H_2, N_2, CO, and CO_2 at high pressure.

2.2. *Characterization of OPF feedstock*

In the simulation environment, biomass is modeled as a non-conventional solid. To facilitate reaction kinetics in the Hysys environment, the feedstock is thermally decomposed into its constituent components. The OPF composition is based on a dry ash-free basis (daf) taken from Sonjaya et al. [36].

Based on elemental analysis, the chemical formula can be determined by calculation [37]. In 100 grams of biomass, there are 48.45 grams of carbon. The mass in grams divided by the molecular weight of carbon (12 g/mol) will result in 4.04 moles of carbon. The same is applied to the other elements, resulting in the following chemical formula for the biomass OPF: $C_{4.04}$ $H_{5.68}$ $O_{3.77}$ $N_{0.02}$ $S_{0.01}$, and this chemical formula was used as input to Aspen Hysys as a hypothetical solid component. The biomass input to Aspen Hysys was assumed to be in pellet form, so pretreatment is not required.

Further, based on Fig. 2 and 3, the processes that occur broadly consist of gasification, synthetic gas (syngas) purification, and ammonia synthesis. Fig. 2 illustrates the interconnection between the gasification process, syngas cleaning, shift conversion, and ammonia synthesis units. Fig. 3 depicts the simulation topology, including logical operators (Recycle, Adjust) and specific unit specifications used to solve the mass and energy balances. The gasification reactions involved in the gasifier, based on data from the study by Heryadi et al. [38], the conversion reactions of the resulting syngas (H_2) are shown in (1) [39].

$$N_2 + 3H_2 \leftrightarrow 2NH_3 \quad (1)$$

2.3 Process description

The plant topology, as illustrated in the Process Flow Diagrams in Figures 2 and 3, is divided into five main sections:

1. Gasification Section: OPF is fed into a circulating fluidized gasifier (CFB) where partial oxidation of the OPF biomass occurs using oxygen and steam as oxidants. The gasification unit

is modeled as an equilibrium reactor to maximize carbon conversion to raw syngas ($CO + H_2$). The gasifier uses steam and oxygen as the gasifying agent/oxidant, respectively. Oxygen is supplied through a cryogenic air separation unit (ASU) that separates oxygen and nitrogen. Oxygen and nitrogen purity are assumed to be 100%. The composition of the syngas produced by gasification was calculated based on equilibrium at 900°C. The process is assumed to be isothermal during the gasification reaction [40]. Waste heat from the reactor can be used for steam generation because the reactor is cooled with water, which converts the waste heat into steam to supply the gasification oxidant. From the CFB gasifier, the output syngas is cooled to 400°C before entering the Water Gas Shift (WGS) reactor to increase the hydrogen content required for ammonia synthesis [41]. A detailed explanation of the gasification process is based on a study conducted by Heryadi et al. [38]. Given the complexity of the biomass gasification reaction, which involves hundreds of side reactions, the gasifier unit is modeled using the Gibbs Free Energy Minimization (equilibrium reactor) approach. In this approach, the composition of the output syngas (primarily CO, H_2, CO_2, CH_4) is calculated to minimize the system's Gibbs energy at 900°C and a specified pressure, without requiring reaction-kinetics data. An isothermal assumption is applied to simplify the reactor temperature profile, assuming the exothermic reaction heat is directly used to generate steam around the reactor wall (water wall), which is modeled as an outgoing energy flow (heat duty).

2. Syngas Cleaning and Conditioning: Water separation and syngas cleaning: Syngas purification from moisture is simulated by modeling the V-100 water separator as a dryer. Acid gases such as H_2S and CO_2 are separated by modeling the X-104 and X-105 splitter components as MEA scrubbers [42]. The dryer reduces the moisture content of the syngas to less than 1 mol%, which is an acceptable level. It removes approximately 90% of the CO_2 and 100% of the H_2S [37]

3. Water Gas Shift (WGS): The cleaned syngas enters the WGS reactor, where carbon monoxide reacts with steam to produce additional hydrogen, adjusting the H_2/N_2 ratio to an appropriate level of approximately 3 to 1 for ammonia synthesis feedstock [43].

4. **Purification**: The sweet syngas undergoes purification, simulated by component splitters (simulated PSA) representing a Pressure Swing Adsorption (PSA) unit to remove CO, CO_2, and sulfur compounds (H_2S) [44,45], producing a high-purity hydrogen stream necessary for ammonia synthesis, especially since these gases are toxic to catalysts and can cause fouling of iron-based catalysts and ultimately lead to catalyst deactivation [46].

5. Ammonia Synthesis Loop: High-purity hydrogen is mixed with nitrogen (3:1 stoichiometric ratio). Nitrogen is assumed to be obtained from ASU. This mixture is compressed (K-100) and fed to the synthesis reactor, which is modelled as an equilibrium reactor. Unreacted gas is recycled, while the ammonia product is condensed and separated at low temperature (vessel V-101). The ammonia synthesis process configuration is based on Ramadhan et al. [47], with minor modifications, including the addition of a control valve (VLV-100) to reduce the operating pressure by 100 bar. The NH3 reactor is modeled as isothermal, since the ammonia formation reaction is exothermic. The operating pressure for simulation in the ammonia reactor is 241 bar, and the temperature is 500 °C [39].

2.4 Simulation basis and assumptions

To ensure the model's convergence and reproducibility while reflecting realistic industrial constraints, the simulation was governed by specific thermodynamic boundaries and operating assumptions. These parameters, along with their physicochemical rationale and supporting literature, are detailed below.

1. Overall system (gasification, WGS, and NH3 Synthesis) is assumed in steady-state conditions, which neglects the dynamic accumulation and is quite common to be implemented for process simulation [38,40,48], and ignores dynamic fluctuations during start-up and shut-down.
2. OPF feedstock is assumed to be homogeneous pellet feed. Homogeneous pellets simplify complex solid modelling in Hysys [36].
3. The gasifier is assumed to use a Gibbs Equilibrium reactor where the process itself is assumed to be isothermal at 900 °C [38,42]. By minimizing Gibbs free energy, the theoretical maximum syngas yield can be obtained without requiring reaction kinetic data, which is quite intensive computationally for complex biomass.
4. The oxidant/ gasifying agent. Oxygen, as a gasifying agent, is assumed to be 100% pure. The maximum purity represents the ideal ASU and is commonly used in gasification simulations [42,49].
5. Syngas cleaning unit. Modelled as a splitter, the separation efficiencies for H_2S and CO_2 are 100% and 90%, respectively [37,42]. Using a splitter, the efficiency of physical absorption solvents (Rectisol/Selexol) was simulated, especially for preliminary mass balance calculations.
6. WGS Reactor. The reaction was assumed to be at equilibrium, and an adequate catalyst volume was assumed to overcome kinetic barriers, ensuring the H_2/N_2 ratio reached 3:1 [50].
7. Purification. The purification of H_2 was modeled using a splitter/separator in Hysys, resulting in high-purity H_2. CO_2, CO, and remaining sulfur compounds are assumed to be 100% removed in this simulation to achieve high-purity H_2 as a feed for ammonia synthesis. Some process simulation studies employed a component splitter in Hysys or a Separator in Aspen Plus to represent a PSA unit [44,51].
8. Compressors. It was assumed to have an isentropic efficiency of 75%. The assumption reflects realistic polytropic behavior in industrial multi-stage centrifugal compressors, preventing underestimation of power duty [48].
9. Ammonia synthesis loop. The reactor was assumed to be isothermal, with an operating temperature of 500 °C and a pressure of 241 bar. This assumption simplifies the temperature profile of the highly exothermic reaction, assuming efficient inter-stage cooling to maintain optimal equilibrium conversion [39,47].
10. Hydrodynamics. Negligible pressure drop simplifies the momentum balance, allowing focus on mass and energy flow. In general, this assumption is common in process simulations that focus on mass and energy balances [42,47,49].

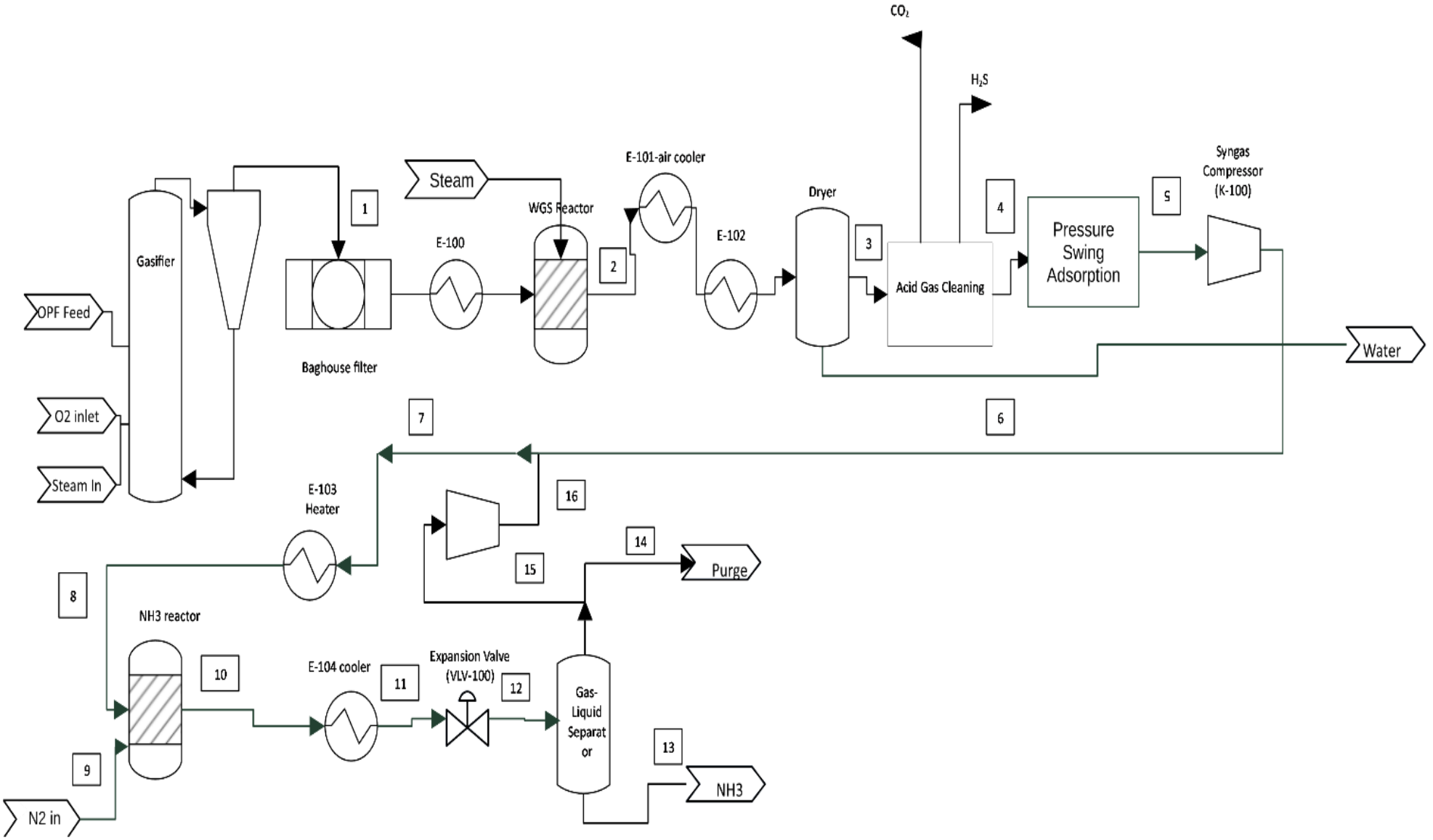

Fig. 2. Schematic process flow diagram (PFD) of the green ammonia plant

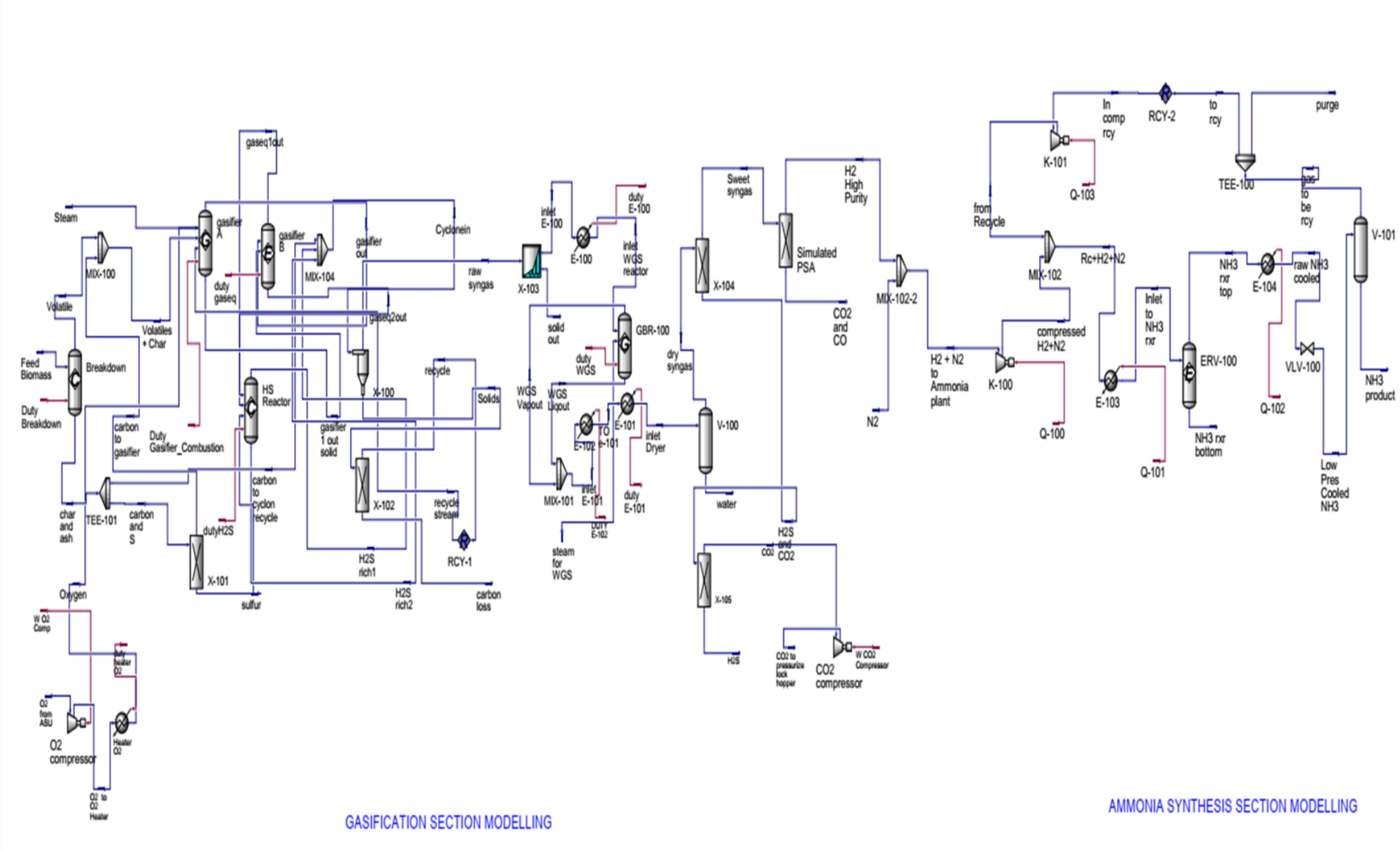

Fig. 3. Detailed aspen HYSYS simulation flowsheet

3. Result and Discussion

3.1. Simulation results

The simulation results are presented in Table 1, where the material streams shown relate only to the model's input and output, and the stream numbers correspond to Figures 2 and 3.

Table 1. Ammonia synthesis material stream using OPF as raw material

Parameter	*Unit*	OPF Feed	raw syngas (1)	Sweet syngas (4)	H_2 High Purity (5)	NH_3 product (13)
Vapor Fraction		0.00	0.99	1.00	1	0.00
Temp.	*°C*	25	900	25	26.	5.42
Pressure	*kPa*	1,000	999.88	599	599	14100
Mole flow rate	*kgmole/h*	139.03	1,279	839	757	495
Mass flow rate	*kg/h*	16,000	24,876	4,813	1,686	8,381
Vol. flow rate (Liq)	*m^3/h*	10.69	40.55	25.72	21.90	13.76
Energy flow	*GJ/h*	283.15	-148.11	-25.13	-1.33	-34.47

Based on Table 1, with an OPF input feed rate of 16,000 kg/h, the ammonia production rate is 8,381 kg/h. The ratio of OPF to ammonia produced is 1.9:1. This result is still within the range of similar studies for feedstock from biomass and coal, where several studies have provided quite diverse ratio results, ranging from 1.81 to 2.71 tonnes of biomass per tonne of ammonia produced with quite diverse dry biomass raw materials, ranging from dry sawdust of pine wood to wood biomass in general [21,31,52]. By converting the OPF feed basis from daf to a wet or as-received basis based on data provided by Sonjaya et al. [36], where the initial moisture content is 8.39% and ash content is 4.29%, from 16,000 kg/h of OPF daf becomes 18,320 kg/h of as-received OPF biomass, the ratio becomes 2.28 (2.28 tonnes of OPF biomass to 1 tonne of ammonia). Based on the biomass feed range above, the simulation results, when converted to an as-received basis, remain within the range of biomass-to-ammonia conversion ratios reported in several previous studies. It is critical to contextualize this thermodynamic result against logistical realities. The simulated capacity represents a small-to-medium-scale plant. Scaling this ratio to a world-scale facility with a larger scale, e.g., more than 1500 tonnes/day, would require over 140,000 kg/h of OPF. This logistical challenge is likely prohibitive given the low bulk density and dispersed generation of OPF compared to pipeline-fed natural gas. Thus, the feasibility of this 1.9:1 yield is strictly tied to decentralized, localized production models rather than centralized mega-plants.

The final ammonia product obtained from the simulation results has a purity of 97.18%. This purity percentage aligns with simulation results from previous studies, which report purities ranging from 95% to above 99% [21,52]. It is important to note that commercial specifications for ammonia are typically defined by weight rather than mole fraction [53]. Due to the difference in molecular weight between ammonia (17 g/mol) and the lighter dissolved synthesis gases (H_2 and N_2, average molecular weight = 8.5 g/mol), the obtained mole purity translates into a much higher mass purity. Theoretical conversion shows that 97.18 mol% corresponds to approximately 98.57 wt%. The 2.82 mol% impurity consists of non-condensable gases (N_2, H_2) that are physically dissolved in the liquid phase at the separator's high operating pressure [54]. More critically, the synthesis loop utilizes iron-based catalysts that are extremely sensitive to poisoning by CO, CO_2, and sulfur [31]. While the Hysys model successfully separates bulk contaminants, the practical risk of trace tar slip and organic sulfur from OPF biomass gasification remains a significant operational threat [55]. Unlike the clean syngas from methane reforming, biomass-derived syngas requires rigorous multi-stage cleaning to ensure impurities remain below the limit required to prevent irreversible catalyst deactivation [20,31].

3.2. Energy conversion efficiency of OPF to ammonia

The energy conversion of the simulated plant is shown in Table 2. The input energy of the OPF biomass is compared with the energy output in ammonia.

Table 2. Efficiency of OPF energy conversion to ammonia

Parameter	Unit	Value
OPF feed mass flow rate	kg/h	16,000
LHV OPF	MJ/kg	17.69
NH_3 product mass flow rate	kg/h	8,381
LHV NH_3	MJ/kg	18.6
Energy Conversion Efficiency of OPF to ammonia	%	55

Based on Table 2, approximately 55% of the energy in OPF is converted to ammonia. It can be said that the energy conversion efficiency of 55% from OPF biomass to ammonia falls within the range of process models or simulations with minimal heat losses, as compared to the results of Gilbert et al. [21] which is 34%. Although the energy conversion efficiency of 55% is competitive with that reported by Gilbert et al. [21], it is important to highlight the factors underlying this high efficiency. The high LHV value of product ammonia, that is, 18.6 MJ/kg, compared to feed woody biomass, as well as the minimal heat loss in the simulation assumptions, contribute significantly to this value. The energy conversion efficiency from this study is quite close to the 56% efficiency reported in the simulation study by Rossetti et al. [52], using pine sawdust LHV data from Gendek [56]. There is a slight difference in energy efficiency between this study and that by Rossetti et al. [45], likely due to differences in feedstock characteristics. OPF has an initial moisture content of 8.39% and a significant ash content of 4.29%, which thermodynamically burdens the gasification process compared to the pine sawdust used in the comparative study. This indicates that although OPF is a waste product, its fuel characteristics are well-suited to conversion, provided moisture content is effectively managed through drying.

Although the conversion efficiency is consistent with general woody biomass studies by Rossetti et al. [52], OPF possesses unique physicochemical properties that the equilibrium model does not fully account for. Specifically, the high potassium content in OPF ash facilitates the formation of

sticky alkali-silicates with low melting points [57,58]. Although the simulation assumes a steady-state gasification temperature of 900°C, operating at this temperature risks severe bed agglomeration and defluidization [59]. In practice, mitigating these risks by lowering operating temperatures or adding additives would likely reduce cold-gas efficiency and carbon conversion. Consequently, the actual biomass-to-ammonia energy efficiency may be lower than the simulated values.

3.3. Energy analysis

The energy released in the exothermic process is summarized in Table 3, based on the process flow diagrams shown in Figures 1 and 2.

Table 3. Waste heat energy that can be used to generate steam

Equipment Description	Energy Stream Name	Energy Stream (GJ/h)
Gasifier	Gasifier duty	-77
WGS Reactor	Duty WGS	-13
Syngas outlet WGS reactor cooler	Duty E-101 & E-102	-75
Raw NH_3 cooler	Q-102	-82
NH_3 Reactor	Q-104	-26

The system's thermal efficiency is significantly influenced by the heat load on the gasifier and the energy released during the exothermic ammonia synthesis reaction. Table 3 shows that thermal outflow occurs due to both cooling and exothermic reactions in the WGS and NH_3 reactors. This outflow of heat can generate steam, which can be used not only as an oxidizing agent or as input to the WGS reactor but also to generate electricity [42].

Table 4 displays the electricity consumption of the leading equipment or operating units in the ammonia production process simulation. Pumps and compressors typically use electric motors, which consume significant electrical energy. The ammonia production process is energy-intensive, particularly in the compression section before entering the ammonia production process and in supporting units such as the ASU and CO_2 compression.

Table 4. Electricity consumption of the main operating unit

Equipment Description	Energy stream ID	Power (kJ/h)	Power (kW)
Oxygen compressor (ASU)	W O_2 Comp	1,003,578	279
CO_2 compressor (Product)	W CO_2 Compresso r	279,692	78
NH_3 feed compressor	Q-100	22,809,692	6,336
Recycle compressor	Q-103	6,974,084	1,937
Total		**31,067,046**	**8,630**

Based on Table 4, the most significant electrical power consumption for driving the compressor is the Feed compressor in the ammonia production process, which requires 6,336 kW. In second place, the recycle compressor for the ammonia production process requires 1,937 kW of power. This large power consumption requires a substantial electrical energy supply. In addition to relying on the primary grid from the national power plant, efforts to save electricity or energy can be made by converting waste heat presented in Table 3 into steam, which can then be used to drive the power plant turbine.

Table 5 shows the plant's key performance indicators. With an ammonia production of 8,381 kg/h, the specific energy consumption can be calculated.

Table 5. Specific energy consumption of OPF-based ammonia

Parameter	Value	Unit
Ammonia produced	8,381	kg/h
Electrical power consumption based on simulation	8,630	kW
Specific energy consumption	**1.03**	**kWh / kg NH_3**

The specific energy consumption of 1.03 kWh/kg NH_3 reflects the high energy requirements for gas compression from the low pressure of the gasification process to the ammonia synthesis pressure of 241 bar. However, total electricity consumption is not considered; only the electricity consumption of the few compressors used in this production process simulation is considered. Several other studies have reported higher specific energy consumption values of 8–12 kWh/kg NH_3 [60,61]. These higher values indicate more detailed energy calculations for processes such as the ASU and PSA, as well as other parts of the ammonia plant that require electricity.

This specific energy consumption value of 1.03 kWh per kg ammonia represents the power requirements for syngas compression, the ammonia synthesis cycle, and cooling, excluding the ASU and the PSA unit. Compared with the existing literature, this value is consistent with the high compression requirements characteristic of biomass gasification. According to Rouwenhorst et al. [62], the theoretical minimum work for the compression and circulation of syngas is approximately 0.1–1.7 kWh/kg NH_3. The obtained value of 1.03 kWh/kg does not reflect the total electricity consumption of the ammonia plant, but rather the compression, cooling, and desorption work [62]. The finding of a specific energy consumption of 1.03 kWh/kg NH_3 for the compression and synthesis sections highlights a significant challenge in ammonia production through biomass gasification, primarily due to the pressure disparity. Gasification occurs at relatively low pressures around 10 bar, while ammonia synthesis absolutely requires high pressure, at 241 bar in this study.

While the calculated specific energy consumption of 1.03 kWh/kg demonstrates the thermodynamic potential of the core synthesis loop, it must be interpreted within the constraints of the simulation's ideal assumptions. In industrial practice, thermodynamic and kinetic limitations in the ammonia synthesis converter result in low single-pass conversion rates, typically 25–30% [63]. This necessitates high recycle rates to compensate for the inevitable pressure drops of 5 to 20 bar across the catalyst bed, which significantly increases the synthesis loop

compression duty [64]. Furthermore, a comprehensive plant boundary assessment that expands the boundary to include the energy-intensive ASU and PSA would eventually enable calculation of the total plant energy intensity closer to the commercial standard of 8–12 kWh/kg NH_3 [61,62].

Simulation data also shows that the feed compressor (Feed Compressor K-100) accounts for 6,336 kW of power consumption. This confirms that the energy-consuming process is not due to the chemical reaction, but instead to the compression process. Therefore, future energy integration scenarios should not only focus on heat recovery from exothermic reactors but also consider a steam turbine drive for the K-100 compressor, utilizing the massive waste heat of -77 GJ/h from the gasifier and -26 GJ/h from the ammonia reactor.

4. Conclusion

This study validates the technical feasibility of converting OPF into green ammonia through integrated process simulations. With a mass conversion ratio of 1.9:1 and an energy conversion efficiency of 55%, OPF can be considered as a viable alternative feedstock candidate for ammonia production. The final product quality reaches 97.18 mol%, or approximately 98.57 wt%, in accordance with industry standards and meeting requirements for fuel and chemical industry applications. However, this process is identified as energy-intensive during syngas compression, which accounts for the most significant power load in plant operation. Furthermore, the specific energy consumption for the synthesis and compression sections is calculated at 1.03 kWh/kg NH_3. Despite this, the figure reflects the theoretical minimum for the compression and synthesis sections only. A comprehensive plant boundary assessment, inclusive of auxiliary units such as the ASU and PSA, must be conducted to obtain a value closer to the industry commercial standard. Collectively, these results confirm that the proposed OPF-based ammonia plant design is promising and warrants further development and study. Key focus for future optimization is heat integration between the gasification reactor and the exothermic ammonia reactor, enabling the production of usable electricity to meet the energy needs of an OPF-based ammonia plant, and also detailing the calculations of the energy consumption of the ASU and PSA unit. Furthermore, a techno-economic study is needed to assess the economic feasibility of OPF-based ammonia production. This study can also be used as part of the support to the Indonesian government's national hydrogen and ammonia roadmap.

5. Acknowledgement

Universitas PGRI Kalimantan primarily supported this research. The authors are grateful to Universitas PGRI Kalimantan for the internal research grant supporting this article.

References

[1] R. Heryadi and B. Widianarko, bio-dimethyl ether from oil palm empty fruit bunch and sustainability assessment of bio-dimethyl ether: a case study in indonesia, *Curr. Appl. Sci. Technol.* 22 (2022).

[2] C.S. Goh and L. Potter, transforming borneo from land exploitation to sustainable development, Yusof Ishak Institute, Singapore, 2023.

[3] P. Basu, biomass gasification and pyrolysis, Elsevier, Burlington, Massachusets, 2010.

[4] A. Van der Drift and H. Boerrigter, synthesis gas from biomass for fuels and chemicals, 2005.

[5] F.A. Rahmatullah, T. Pamungkas, S. Mutia, Z. Zulfansyah and H. Rionaldo, simulation of dimethyl ether production as lpg substitute using lng from arun terminal with tri-reforming and direct synthesis method, *Konversi* 13 (2024) 11–15.

[6] M. Alnajideen, H. Shi, W. Northrop, D. Emberson, S. Kane, P. Czyzewski, et al., ammonia combustion and emissions in practical applications: a review, *Carbon Neutrality* 3 (2024).

[7] D.R. MacFarlane, P.V. Cherepanov, J. Choi, B.H.R. Suryanto, R.Y. Hodgetts, J.M. Bakker, et al., a roadmap to the ammonia economy, *Joule* 4 (2020) 1186–1205.

[8] B. Mohanty and V.K. Singh, performance of explosives and new developments, 2012.

[9] R. Heryadi, J.D.H. Utama and A.V. Prasmoro, cost and fragmentation prediction of ammonium nitrate fuel oil versus bulk emulsion explosives, *IOP Conf. Ser. Earth Environ. Sci.* 1422 (2024).

[10] B.F. Tchanche, M. Pétrissans and G. Papadakis, heat resources and organic rankine cycle machines, *Renew. Sustain. Energy Rev.* 39 (2014) 1185–1199.

[11] M. Azuan, study and development of pellet fuel from oil palm frond, Universiti Teknologi Petronas, 2008.

[12] M.S. Sirrajudin, M.S.M. Rasat, R. Wahab, M.H.M. Amini, M. Mohamed, M.I. Ahmad, et al., enhancing the energy properties of fuel pellets from oil palm fronds of agricultural residues by mixing with glycerin, *ARPN J. Eng. Appl. Sci.* 11 (2016) 6122–6127.

[13] W. Wattana, S. Phetklung, W. Jakaew, S. Chumuthai, P. Sriam and N. Chanurai, characterization of mixed biomass pellet made from oil palm and para-rubber tree residues, *Energy Procedia* 138 (2017) 1128–1133.

[14] F. Abnisa, A. Arami-Niya, W.M.A. Wan Daud, J.N. Sahu and I.M. Noor, utilization of oil palm tree residues to produce bio-oil and bio-char via pyrolysis, *Energy Convers. Manag.* 76 (2013) 1073–1082.

[15] N.N. Omar, N. Abdullah, I.S. Mustafa and F. Sulaiman, characterisation of oil palm frond for bio-oil production, *ASM Sci. J.* 11 (2018) 9–22.

[16] N. Sareekam, S.K. Kamarudin and N.H. Kasmuri, optimization of bio oil from palm oil fronds via fast pyrolysis, *Indian J. Sci. Technol.* 9 (2016).

[17] H.A. Umar, S.A. Sulaiman, R.K. Ahmad and S.N. Tamili, characterisation of oil palm trunk and frond as fuel for biomass thermochemical, *IOP Conf. Ser. Mater. Sci. Eng.* 863 (2020).

[18] X.O. Zhong, P.T. Yi, B. Kunasundari and H.S. Siew, oil palm frond as a sustainable and promising biomass source in malaysia: a review, *Environ. Prog. Sustain. Energy* 00 (2017) 1–11.

[19] W.M.S.W. Ismail, T. Mohd Thaim and R. Abdul Rasid, biomass gasification of oil palm fronds (opf) and koompasia malaccensis (kempas) in an entrained flow gasifier: a performance study, *Biomass Bioenergy* 124 (2019) 83–87.

[20] J. Andersson and J. Lundgren, techno-economic analysis of ammonia production via integrated biomass gasification, *Appl. Energy* 130 (2014) 484–490.

[21] P. Gilbert, S. Alexander, P. Thornley and J. Brammer, assessing economically viable carbon reductions for the production of ammonia from biomass gasification, *J. Clean. Prod.* 64 (2014) 581–589.

[22] E. Gençer, G.R. Burniske, O.C. Doering, W.E. Tyner, R. Agrawal, W.N. Delgass et al., sustainable production of ammonia fertilizers from biomass, *Biofuels Bioprod. Biorefin.* 14 (2020) 725–733.

[23] M. Martín and A. Sánchez, biomass pathways to produce green ammonia and urea, *Curr. Opin. Green Sustain. Chem.* 47 (2024) 100933.

[24] G. Mallouppas, C. Ioannou and E.A. Yfantis, a review of the latest trends in the use of green ammonia as an energy carrier in maritime industry, *Energies* 15 (2022).

[25] L. Zhai, S. Liu and Z. Xiang, ammonia as a carbon-free hydrogen carrier for fuel cells: a perspective, *Ind. Chem. Mater.* 1 (2023) 332–342.

[26] F. Schüth, challenges in hydrogen storage, *Eur. Phys. J. Spec. Top.* 176 (2009) 155–166.

[27] R. Nabila, W. Hidayat, A. Haryanto, U. Hasanudin, D.A. Iryani, S. Lee et al., oil palm biomass in Indonesia: thermochemical upgrading and its utilization, *Renew. Sustain. Energy Rev.* 176 (2023).

[28] Thyssenkrupp, green ammonia revolutionizes the transport of hydrogen, 2024.

[29] R. Heryadi, J.D.H. Utama, I.P. Hikariantara and M. Saufi, green ammonia production potential prediction from oil palm frond waste in the Kalimantan region, *IOP Conf. Ser. Earth Environ. Sci.* 1562 (2025).

[30] P. Arora, A.F.A. Hoadley, S.M. Mahajani and A. Ganesh, multi-objective optimization of biomass based ammonia production - potential and perspective in different countries, *J. Clean. Prod.* 148 (2017) 363–374.

[31] P. Arora, A.F.A. Hoadley, S.M. Mahajani and A. Ganesh, small-scale ammonia production from biomass: a techno-enviro-economic perspective, *Ind. Eng. Chem. Res.* 55 (2016) 6422–6434.

[32] Ministry of Energy and Mineral Resources, peta jalan hidrogen dan amonia nasional, 2025.

[33] C. Chotimah, N.N. Syafitri and K. Udyani, absorber design simulation for CO2 using K2CO3 absorbent with Aspen Hysys V.10 software, *Konversi* 11 (2022) 119–124.

[34] J.J.Y. Lim, S.W. Ching, Y.Y. Tan, Z.R. Goh, S.W. Chang and N. Mohd, co-gasification of palm oil EFB and MSF for renewable hydrogen production: a conceptual design and simulation, *Malaysian J. Chem.* 26 (2024) 211–232.

[35] A.A. Widyadhana, D.J.G. Siahaan, F.F. Verlanda and M.A.D. Rahman, improving mass efficiency in ammonia production from hydrogen and nitrogen through optimizing operating condition, *J. Chem. Eng. Res. Prog.* 1 (2024) 91–96.

[36] A.N. Sonjaya, P. Zuldian, A.S. Auzani, Y. Widyawati, Cahyadi, N. Nisfah et al., experimental study of syngas production from oil palm frond gasification based on bubble cap air distributor at low temperature, *Case Stud. Chem. Environ. Eng.* 11 (2025) 101143.

[37] H. Florence and A. Bour, modelling and optimization of a process from biomass to liquid fuels via Fischer-Tropsch synthesis, Norwegian University of Science and Technology, 2016.

[38] R. Heryadi, A.S. Uyun, E. Yandri, S.M. Nur and K. Abdullah, palm empty fruit bunch gasification simulation in circulating fluidized bed gasifier, *E3S Web Conf.* 67 (2018) 02043.

[39] M. Farsi, ammonia production from syngas: plant design and simulation, *Adv. Synth. Gas Methods Technol. Appl.* 4 (2022) 381–399.

[40] W. Doherty, A. Reynolds and D. Kennedy, simulation of a circulating fluidised bed biomass gasifier using ASPEN Plus: a performance analysis, Dublin Institute of Technology, 2008.

[41] A.M. Parvez, T. Wu, S. Li, N. Miles and I.M. Mujtaba, bio-DME production based on conventional and CO2-enhanced gasification of biomass: a comparative study on exergy and environmental impacts, *Biomass Bioenergy* 110 (2018) 105–113.

[42] R. Heryadi, A.S. Uyun, E. Yandri, S.M. Nur and K. Abdullah, single stage dimethyl ether plant model based on gasification of palm empty fruit bunch, *IOP Conf. Ser. Mater. Sci. Eng.* 532 (2019).

[43] M.Y. Aslan, J.S.J. Hargreaves and D. Uner, the effect of H2:N2 ratio on the NH3 synthesis rate and on process economics over the Co3Mo3N catalyst, *Faraday Discuss.* 229 (2021) 475–488.

[44] S. Sarkar, A. Kumar and A. Sultana, biofuels and biochemicals production from forest biomass in Western Canada, *Energy* 36 (2011) 6251–6262.

[45] P. Tuna, C. Hulteberg and S. Ahlgren, techno-economic assessment of nonfossil ammonia production, *Environ. Prog. Sustain. Energy* 33 (2014) 1290–1297.

[46] C. Smith, A.K. Hill and L. Torrente-Murciano, current and future role of Haber-Bosch ammonia in a carbon-free energy landscape, *Energy Environ. Sci.* 13 (2020) 331–344.

[47] D.P. Ramadhan, F.K.T. Hutasoit, G.A. Primaditya, M.V. Aurielly and M.Y.Z. Muafi, improving energy efficiency in ammonia production from hydrogen and nitrogen through optimizing operating condition, *J. Chem. Eng. Res. Prog.* 2 (2025) 210–215.

[48] M. Peters, K. Timmerhaus, R. West and M. Peters, plant design and economics for chemical engineers, 2003.

[49] L.R. Clausen, B. Elmegaard and N. Houbak, technoeconomic analysis of a low CO2 emission dimethyl ether (DME) plant based on gasification of torrefied biomass, *Energy* 35 (2010) 4831–4842.

[50] P. Ebrahimi, A. Kumar and M. Khraisheh, a review of recent advances in water-gas shift catalysis for hydrogen production, *Emergent Mater.* 3 (2020) 881–917.

[51] P. Tunå and C. Hulteberg, woody biomass-based transportation fuels - a comparative techno-economic study, *Fuel* 117 (2014) 1020–1026.

[52] I. Rossetti, A. Tripodi, M. Tommasi and G. Ramis, conceptual design of a process for hydrogen production from waste biomass and its storage in form of a liquid ammonia, *Int. J. Hydrogen Energy* 48 (2023) 37443–37460.

[53] J. Atchison, a fuel standard for ammonia: panel wrap-up from the ammonia energy conference 2020, 2020.

[54] V. Pattabathula and J. Richardson, introduction to ammonia production, *Chem. Eng. Prog.* 112 (2016) 69–75.

[55] A. Jayanarasimhan, R.M. Pathak, A.M. Shivapuji and L. Rao, tar formation in gasification systems: a holistic review of remediation approaches and removal methods, *ACS Omega* 9 (2024) 2060–2079.

[56] A. Gendek, combustion heat and calorific value of the mix of sawdust and cones of common pine (Pinus sylvestris L.), *Ann. Warsaw Univ. Life Sci. SGGW Agric.* 66 (2015) 137–144.

[57] T. Kittivech and S. Fukuda, effect of bed material on bed agglomeration for palm empty fruit bunch (EFB) gasification in a bubbling fluidised bed system, *Energies* 12 (2019).

[58] P. Shrivastava, P. Khongphakdi, A. Palamanit, A. Kumar and P. Tekasakul, investigation of physicochemical properties of oil palm biomass for evaluating potential of biofuels production via pyrolysis processes, *Biomass Convers. Biorefin.* 11 (2020) 1987–2001.

[59] P. Lahijani, G.D. Najafpour, Z. Alimuddin and M. Mohammadi, air gasification of palm empty fruit bunch in a fluidized bed gasifier using various bed materials, *World Renew. Energy Congr.* (2011).

[60] T. Brown, round-trip efficiency of ammonia as a renewable energy transportation media, 2017.

[61] G. de la Hera, G. Ruiz-Gutiérrez, J.R. Viguri and B. Galán, flexible green ammonia production plants: small-scale simulations based on energy aspects, *Environ.* 11 (2024).

[62] K.H.R. Rouwenhorst, A.G.J. Van der Ham, G. Mul and S.R.A. Kersten, islanded ammonia power systems: technology review and conceptual process design, *Renew. Sustain. Energy Rev.* 114 (2019).

[63] C. Quintero-Masselski, J.F. Portha and L. Falk, conception and optimization of an ammonia synthesis superstructure for energy storage, *Chem. Eng. Res. Des.* 177 (2022) 826–842.

[64] M. Appl, ammonia, Wiley-VCH Verlag GmbH & Co. KGaA, 2006.